International Journal of Mass Spectrometry 325–327 (2012) iv–x

Contents lists available at ScienceDirect

International Journal of Mass Spectrometry

journal homepage: www.elsevier.com/locate/ijms

Contents

Foreword

1–2

Foreword

Jean H. Futrell, Alan G. Marshall

3–9

Biography and Publications of Eugene Nikolaev

Alan G. Marshall, Jean H. Futrell

Ion Behavior in Electric and Magnetic Fields

10–18

Sidebands in Fourier transform ion cyclotron resonance mass spectra

Saša M. Miladinović, Anton N. Kozhinov, Oleg Yu. Tsybin, Yury O. Tsybin

► Sidebands of reduced cyclotron frequency harmonics in experimental FT-ICR spectra. ► Evaluation of the existing theory of ICR signal on the basis of the experimental data. ► An analytical model showing the physical origin of sidebands in FT-ICR spectra. ► Sidebands as a result of broadband amplitude-phase modulation occurring in ICR signal.

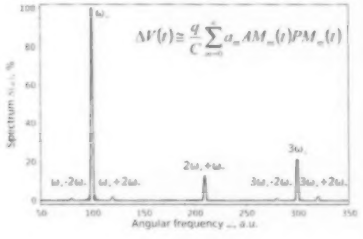

Elsevier B.V.
http://dx.doi.org/10.1016/S1387-3806(12)00319-3

International Journal of Mass Spectrometry 325–327 (2012) iv–x

Contents lists available at ScienceDirect

International Journal of Mass Spectrometry

journal homepage: www.elsevier.com/locate/ijms

Contents

Foreword

1–2

Foreword

Jean H. Futrell, Alan G. Marshall

3–9

Biography and Publications of Eugene Nikolaev

Alan G. Marshall, Jean H. Futrell

Ion Behavior in Electric and Magnetic Fields

10–18

Sidebands in Fourier transform ion cyclotron resonance mass spectra

Saša M. Miladinović, Anton N. Kozhinov, Oleg Yu. Tsybin, Yury O. Tsybin

► Sidebands of reduced cyclotron frequency harmonics in experimental FT-ICR spectra. ► Evaluation of the existing theory of ICR signal on the basis of the experimental data. ► An analytical model showing the physical origin of sidebands in FT-ICR spectra. ► Sidebands as a result of broadband amplitude-phase modulation occurring in ICR signal.

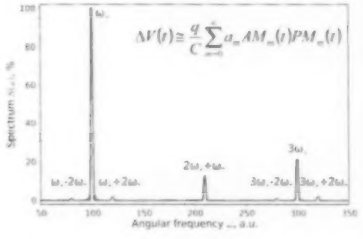

Elsevier B.V.
http://dx.doi.org/10.1016/S1387-3806(12)00319-3

19–24

Analysis of phase dependent frequency shifts in simulated FTMS transients using the filter diagonalization method

Franklin E. Leach III, Andriy Kharchenko, Gleb Vladimirov, Konstantin Aizikov, Peter B. O'Connor, Eugene Nikolaev, Ron M.A. Heeren, I. Jonathan Amster

► Application of filter diagonalization for harmonic inversion of simulated data. ► Simulation of phase dependent frequency shifts in FT-ICR MS and orbital FTMS. ► Analysis of space charge induced frequency shifts in simple and complex systems.

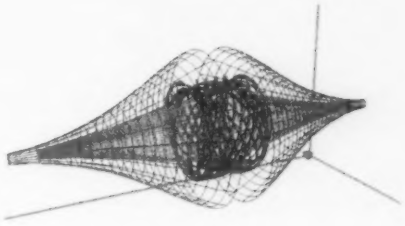

25–29

Prefocusing inside a linear ion beam guide—A SIMION study

Basem Kanawati, Karl Peter Wanczek, Istvan Gebefügi, Philippe Schmitt-Kopplin

► The performance of an ion beam guide was studied by extensive SIMION simulations. ► Ion trajectories were calculated under 1 Pa with HS1 hard sphere collision model. ► Mass dependent transmission efficiency curves in different DC + RF fields were obtained. ► An enhanced operation mode for expanding the range toward lower masses is suggested.

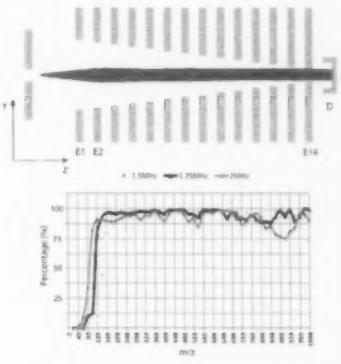

30–44

Theory of simultaneous dipole and quadrupole excitation of the ion motion in a Penning trap

Martin Kretzschmar

► A theoretical description of the excitation of the ion motion in a Penning trap by the simultaneous action of dipolar and quadrupolar radio-frequency fields is developed. ► Equations of motion are set up and their general solution is derived. ► A detailed discussion of SIMCO-excitation (simultaneous dipolar excitation at the magnetron frequency and quadrupolar excitation at the cyclotron frequency) is given. ► The mass resolution of ion purification techniques based on SIMCO-excitation is discussed.

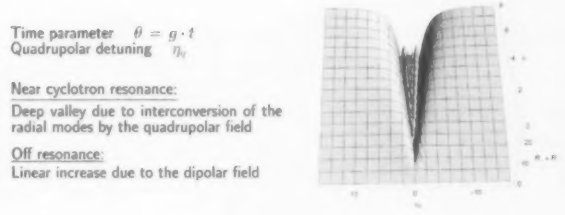
Time parameter $\theta = g \cdot t$
Quadrupolar detuning η_q
Near cyclotron resonance:
Deep valley due to interconversion of the radial modes by the quadrupolar field
Off resonance:
Linear increase due to the dipolar field

45–50

A conceptual approach for FT-ICR cell harmonization utilizing external shim electrodes

Aleksey V. Tolmachev, Errol W. Robinson, Richard D. Smith, Franklin E. Leach III, Jean H. Futrell, Ljiljana Paša-Tolić

► Development of a conceptual approach for FT-ICR cell harmonization. ► Application of external shim electrodes to FT-ICR trapped ion cells. ► Mechanical and electrical simplification of harmonization. ► Evaluation of potential harmonization using normalized radial electric field per radius (E_r/r).

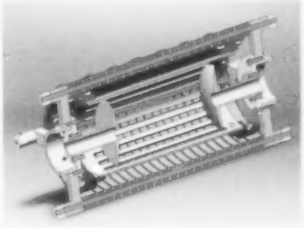

51–57

Buffer-gas-free mass-selective ion centering in Penning traps by simultaneous dipolar excitation of magnetron motion and quadrupolar excitation for interconversion between magnetron and cyclotron motion

M. Rosenbusch, K. Blaum, Ch. Borgmann, S. Kreim, M. Kretzschmar, D. Lunney, L. Schweikhard, F. Wienholtz, R.N. Wolf

► We investigate a new excitation scheme for mass-selective ion centering in Penning traps. ► A dipolar excitation at the ions' magnetron frequency and a quadrupolar excitation at the cyclotron frequency are superimposed. ► We present the theory of the ions' motion and first experimental tests of the new method. ► The experiment yields high resolving powers for mass selection.

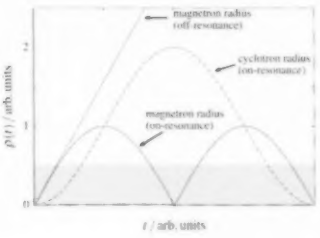

58–66

Perturbation theory for ion motion in quadrupole radio frequency field

Sudakov Mikhail, Apatskaya Maria

► Paper develops perturbation theory for ion motion in quadrupole RF fields. ► First order perturbations for ion coordinated over single RF cycle are obtained. ► Stability parameter of the perturbed motion is defined. ► Boundaries of stability and resolving power of mass filter are defined analytically.

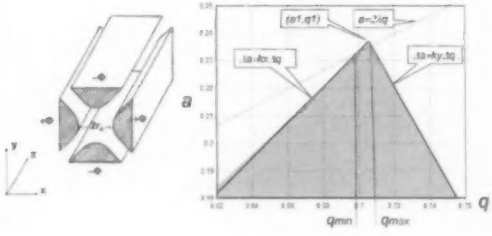

Mass Spectral Analysis

67–72

Baseline correction of absorption-mode Fourier transform ion cyclotron resonance mass spectra

Feng Xian, Yuri E. Corilo, Christopher L. Hendrickson, Alan G. Marshall

► Phasing an FT-ICR mass spectrum achieves up to 2× higher resolution, but introduces baseline "roll". ► Here, we provide an algorithm that eliminates baseline roll. ► Peak-picking, mass resolution, and quantitation are all improved.

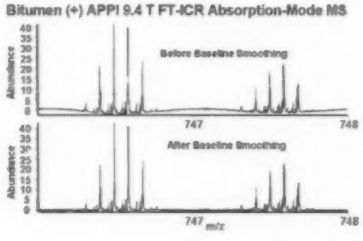

73–79

Self-correlation method for processing random phase signals in Fourier Transform Mass Spectrometry

Y. Melodie Du, Wei Xu, Zheng Ouyang

► A simple algorithm based on self-correlation function has been developed for signal enhancement with data recorded at random phases during the image current measurements. ► The effectiveness of the method has been demonstrated with data of low signal-to-noise ratios (as poor as −40 dB). ► Various ways of implementing the SC method have been developed and demonstrated.

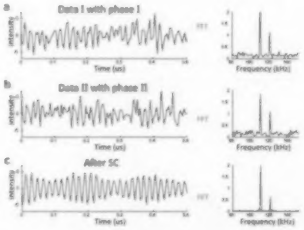

Mass Spectrometry Instrumentation

80–85

Orbitrap mass spectrometry with resolving powers above 1,000,000

Eduard Denisov, Eugen Damoc, Oliver Lange, Alexander Makarov

► Ultra-high resolving power in excess of 1,000,000 using Orbitrap technology. ► Resolution of fine isotopic structure of minor isotopomers of peptides and small molecules. ► Direct identification of coeluting amidated and deamidated forms for mellitin and Substance P peptides. ► Baseline separation of isotopes of transferrin protein.

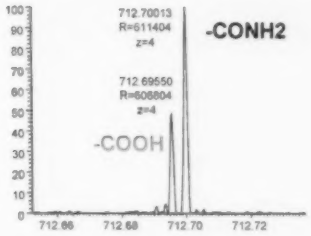

86–94

New way to build a high-performance gas-dynamic interface to produce and transport ions into a mass analyzer

Valeriy V. Raznikov, Vladislav V. Zelenov

► Supersonic gas flow formation inside a capillary is confirmed experimentally. ► The estimated divergence of Ar flow corresponds to the temperature below 0.01 K. ► Divergence of the air flow through capillary corresponds to similar temperature. ► Gas molecules mirror reflection from capillary walls may explain flow properties. ► Two-grid mirror reflection is proposed to record effectively ions from the flow.

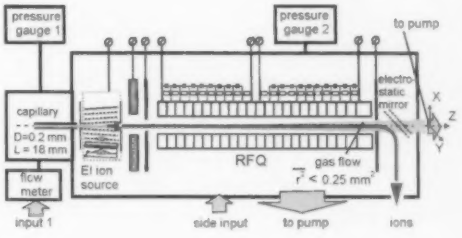

Gas-Phase Ion Chemistry/Fragmentation

95–99

Low energy (0–12 eV) electron driven reactions in linear and cyclic perfluorocompounds

Janina Kopyra, Iwona Szamrej, Stefan Karolczak, Eugen Illenberger

► Electron attachment to C_6F_{14}, $C_6F_{11}CF_3$ and $C_6F_{11}C(O)Cl$ leads to effective decomposition of the molecules in the subexcitation energy range (<3 eV). ► Perfluorocompounds preferentially decompose into closed shell anions of the form $C_nF_{2n+1}^-$. ► The resonance positions for F^- formation show specific features for the three compounds thereby allowing to predict the site from which F^- originates.

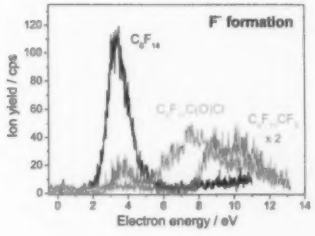

100–112

MALDI mass spectrometry of fullerene derivatives

Vitaliy Yu. Markov, Andrey Ya. Borschevsky, Lev N. Sidorov

► Fragmentation of ions occurs mostly via monomolecular detachment of the addends. This decay requires an interior energy surplus of 7–17 eV. ► Being time-delayed it leads to the appearance of metastable peaks in mass spectra. ► This fact permits to apply MALDI mass spectrometry for identification of radicals. ► The energy surplus pointed to the formation of ions by MALDI in a condensed medium.

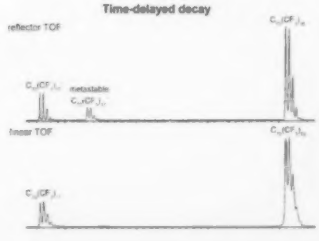

113–120

ECD-like peptide fragmentation at atmospheric pressure

Vadym D. Berkout, Vladimir M. Doroshenko

► The atmospheric pressure fragmentation cell produced ECD-like fragmentation spectra. ► Fragmentation proceeds via capture of free electrons produced in the gas discharge. ► *c*-type and lower charge state molecular ions are mainly observed. ► Peptide phosphorylation group remains intact during fragmentation. ► Ion mobility separation allows for MS/MS-like studies at atmospheric pressure.

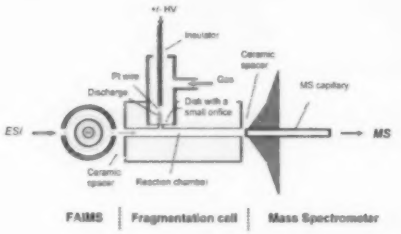

Biological Mass Spectrometry

121–129

Controlled trypsinolysis of human cancer and non-cancer sera for direct matrix-assisted laser desorption/ionization time-of-flight mass spectrometry

Ilya Yu. Toropygin, Olga A. Mirgorodskaya, Sergei A. Moshkovskii, Marina V. Serebryakova, Alexander I. Archakov

► Serum digestion with low trypsin quantities yielded selective hydrolysis of proteins other than albumin. ► This process is suggested to be performed by the trypsin-α_2M complex. ► Direct quantitative MALDI-TOF analysis in serum. ► The serum amyloid A hydrolysis is substantially faster in cancer serum.

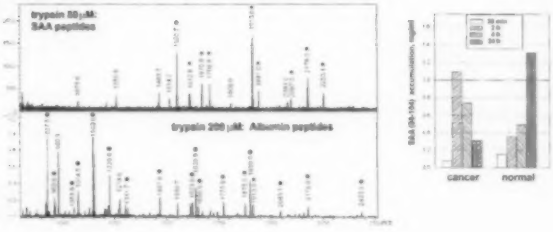

130–1

Top-down hydrogen/deuterium exchange and ECD-stitched FTICR-MS for probing structural dynamics of a 29-kDa enzyme

Jingxi Pan, Jun Han, Christoph H. Borchers

► A new "ECD-stitching" method is demonstrated on a 29 kDa protein, CAII. Results agree with structural features of CAII determined by X-ray crystallography. ► ECD-stitching top-down HDX was also applied to changes induced by drug binding. ► HDX showed changes due to drug binding in distal residues in hinge regions of CAII. ► X-ray studies showed no differences between drug-free and FSM-bound CAII structures.

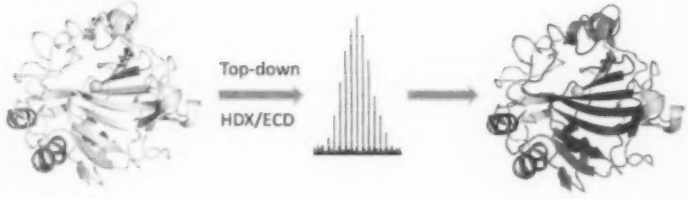

139–149

The influence glutamic acid in protonated $b_3 \rightarrow b_2$ formation from VGEIG and related analogs

Lindsay Morrison, Árpád Somogyi, Vicki H. Wysocki

► b_2 oxazolone formation is shown to be exclusively dependent on a b_3 anhydride intermediate in protonated VGEIG. ► Fragmentation of b_3 to b_2 in this system thus occurs by a single step pathway in which an a_3 ion does not act as an intermediate. ► The b_3 anhydride of protonated VGEIG is shown to play a critical role in the formation of b_3 macrocyclic structures. ► Computational modeling and MS^3 of four sequence isomers additionally suggest that this is an 11-membered macrocycle. ► Alpha proton scrambling is demonstrated by QCID-HDX-SORI on VXEIG analogs. ► MS^3 studies of VG(2,2-d2)EIG and computational modeling demonstrate that scrambling occurs by a multi-step pathway.

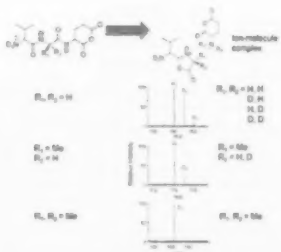

150–160

A multimodal mass spectrometry imaging approach for the study of musculoskeletal tissues

Sanaullah Chughtai, Kamila Chughtai, Berta Cillero-Pastor, András Kiss, Prashant Agrawal, Luke MacAleese, Ron M.A. Heeren

► Multiplexed chemical investigation of tissues affected by Rheumatoid Arthritis. ► Multimodal MS imaging reveals tissue classification. ► Detailed molecular signatures of protein localizations and local interactions. ► Combined lipidome and proteome imaging.

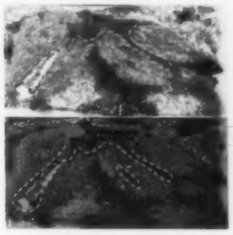

161–166

Signal and charge enhancement for protein analysis by liquid chromatography–mass spectrometry with desorption electrospray ionization

Yan Liu, Zhixin Miao, Rajeswari Lakshmanan, Rachel R. Ogorzalek Loo, Joseph A. Loo, Hao Chen

► Reactive DESI was used as a versatile interface to couple RP-HPLC with MS. ► Supercharging reagents doping in DESI spray to "supercharge" protein eluted from LC. ► Supercharging reagents overcome TFA signal suppression during ionization. ► LC/DESI-MS is a valuable method for protein analysis.

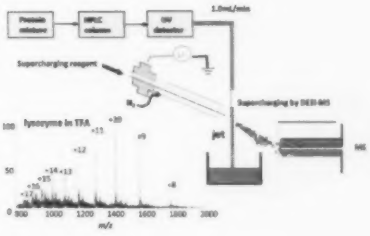

Atmospheric Pressure Ionization Mass Spectrometry

167–171

Spray mechanism in paper spray ionization

Ryan D. Espy, Ariel R. Muliadi, Zheng Ouyang, R. Graham Cooks

► We describe the spray modes during paper spray ionization. ► When solvent-rich, paper spray produces multimodal droplet distributions. ► Solvent-deficient paper spray produces monodisperse drops and a corona discharge. ► Microfiber structures enhance the electric field near the Taylor cone(s).

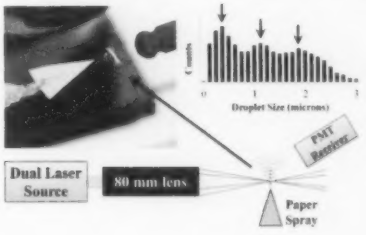

172–182

Ambient molecular imaging of dry fungus surface by electrospray laser desorption ionization mass spectrometry

Min-Zong Huang, Sy-Chyi Cheng, Siou-Sian Jhang, Chih-Chiang Chou, Chu-Nian Cheng, Jentaie Shiea, Igor A. Popov, Eugene N. Nikolaev

► Ambient molecular image of hard and thick fungus slices via ELDI/MS was developed. ► Volatile and nonvolatile compounds in the fungus were simultaneously detected. ► Effects of laser frequency and stage moving speed for image analysis were studied.

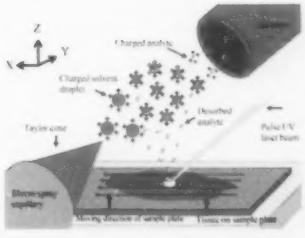

183–188

Mass spectrometric characterization of a dinuclear terbium phthalocyaninato complex

Oliver Hampe, Svetlana Klyatskaya, Tatjana Karpuschkin, Matthias Vonderach, Patrick Weis, Mario Ruben, Manfred M. Kappes
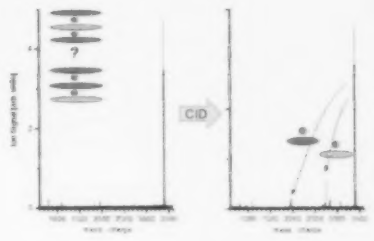
► Newly synthesized neutral heteroleptic bis-terbium-tris-phthalocyaninato sandwich complex electrosprayed as singly and doubly charged anion upon solution phase reduction. ► Stacking configuration determined via collision-induced dissociation experiments and ion-mobility spectrometry. ► For dianionic complex electron emission channel competes with ionic fragmentation upon collisional activation.